Vα14iNKT cell Deficiency Prevents Acetaminophen-Induced Acute Liver Failure by Enhancing Hepatic Glutathione and Altering APAP Metabolism

Isaac Downs[a], **Tak Yee Aw**[a], **Jianfeng Liu**[a], **Patrick Adegboyega**[b], and **Maureen N. Ajuebor**[a,*]

[a]Department of Molecular & Cellular Physiology, Louisiana State University Health Sciences Center-Shreveport Louisiana

[b]Department of Pathology, Louisiana State University Health Sciences Center-Shreveport Louisiana

Abstract

Acetaminophen (APAP) overdose is widely regarded as a major cause of acute liver failure in the United States. Intentional or accidental overdose of APAP in man or rodent elicits direct hepatocellular injury that is accompanied by hepatic depletion of the antioxidant, glutathione (GSH). In recent years, the innate immune response has also been shown to promote the development of APAP hepatotoxicity via indirect liver damage. In the present study, we demonstrate that Jα18$^{-/-}$ mice, which are selectively deficient in the innate immune T cell, Vα14iNKT cells, were resistant to APAP hepatotoxicity relative to WT mice as reflected by biochemical and histological liver injury markers. In parallel, improvement in the biochemical and histological parameters of liver injury in Jα18$^{-/-}$ mice was associated with a significant increase in hepatic levels of GSH, which detoxified APAP metabolites to attenuate hepatic oxidative stress, liver injury and necrosis. Notably, the protective effect of hepatic GSH during Vα14iNKT cells deficiency was demonstrated by its depletion in Jα18$^{-/-}$ mice using DL-buthionine-[*S,R*]-sulfoximine which exacerbated hepatic oxidative and nitrosative stress as well as liver necrosis and caused mice mortality. Extraordinarily, APAP metabolism in Jα18$^{-/-}$ mice was altered in favor of hepatic GSH conjugates and decreased glucuronide conjugates. In summary, we reveal a novel finding establishing a unique association between hepatic innate immunity and GSH levels in altering APAP metabolism to suppress liver injury and necrosis during Vα14iNKT cells deficiency in Jα18$^{-/-}$ mice.

Keywords

Glutathione; APAP; Vα14iNKT cells; ROS; Liver

Correspondence: Dr. Maureen N. Ajuebor, Department of Molecular & Cellular Physiology, LSUHSC-Shreveport, 1501 Kings Highway, LA 71130-3932, USA, Tel: 318 675 4158, majueb@gmail.com.

INTRODUCTION

Globally, acetaminophen (APAP; *N*-acetyl-*p*-aminophenol) is a commonly used analgesic and antipyretic that is generally safe at the recommended dose. Widespread use of APAP in hundreds of prescription and over-the counter drugs has increased the prevalence of APAP hepatotoxicity [1, 2]. Pre-existing liver disease, nutrition, age, genetic polymorphisms, alcohol, tobacco, or interactions with other drugs have been reported to enhance the toxic effects of APAP [1]. For this reason, APAP overdoses are the most common cause of acute liver failure (ALF) in the U.S [1, 2]. APAP intoxication can initiate liver injury by direct and immune-mediated mechanisms [3].

Direct mechanism of APAP induced cell death occurs through the metabolic or oxidative phase [1, 2]. The metabolic phase involves glucuronidation, sulfation, and oxidation pathways. These APAP biotransformation pathways form glucuronide, sulfate, and glutathione conjugates that increase the polarity and solubility of the xenobiotic contributing to excretion. For example, the glucuronidation pathway uses glucuronyl transferases to catalyze UDP-glucuronic acid conjugation to APAP forming APAP-glucuronide whereas the sulfation pathway uses sulfotransferases and the cofactor, 3′-phosphoadenosine-5′-phosphosulfate (PAPS), to add a sulfate group to APAP forming APAP-sulfate [4]. During the oxidation pathway, APAP is oxidized to *N*-acetyl-*p*-benzoquinone imine (NAPQI) catalyzed by cytochrome P450 enzymes (e.g. CYP2E1; an enzyme found in high levels in centrilobular hepatocytes) [2, 5]. NAPQI is an electrophile that forms protein adducts (e.g. mitochondrial proteins) during the metabolic phase of APAP toxicity[2]. Glutathione-*S*-transferase detoxifies NAPQI by catalyzing the conjugation of the antioxidant, glutathione (GSH), to NAPQI to form 3-[glutathione-*S*-yl]-APAP (APAP-GSH) [1, 2]. Therefore, APAP intoxication increases CYP2E1 activity promoting NAPQI accumulation and subsequent hepatic GSH depletion [2, 6]. In summary, the oxidative phase involves mitochondrial dysfunction, which increases reactive oxygen species (ROS) production leading to oxidative/nitrosative stress, ATP depletion, hepatocyte injury, and subsequent centrilobular necrosis.

Immune-mediated liver damage is also evident during APAP overdose. Emerging studies have demonstrated pathophysiological roles for innate immune cells such as peroxynitrite-producing Kupffer cells and neutrophils during APAP hepatotoxicity [2, 7, 8]. Lymphocytes have also been reported to promote the development of APAP liver toxicity as RAG2$^{-/-}$ mice, which are deficient in T and B cells, were found to be resistant to liver injury [9]. Conversely, the adoptive transfer of CD4$^+$ T cells into RAG2$^{-/-}$ mice increased APAP-induced liver damage. More recently, both NKT and NK cells were reported to participate in the development of APAP hepatotoxicity since simultaneous depletion of both cell types suppressed hepatic injury [9–11]. Specifically, CD1d$^{-/-}$ mice which lack both Type I NKT cells (i.e. Vα14*i*NKT cells) and Type II NKT cells were resistant to APAP hepatotoxicity only if NK cells were also depleted [10].

Vα14*i*NKT cells are a major class of NKT cells that constitute 20–40% of the hepatic lymphocyte population [12]. These innate T cells swiftly produce pro-inflammatory cytokines and chemokines on activation [13]. Vα14*i*NKT cells have an invariant T cell receptor with a Vα14-Jα18 chain associated with a Vβ2, Vβ7, or Vβ8.2 chain [13, 14] and are directly stimulated by TCR and TCR-independent mechanisms. The specific role of Vα14*i*NKT cells in the development of APAP hepatotoxicity is incompletely defined. In the present study, we demonstrate that Vα14*i*NKT cells induce pro-inflammatory effects during APAP hepatotoxicity by regulating hepatic GSH production and APAP metabolism.

MATERIALS AND METHODS

Mice

Wildtype (WT) male C57BL/6 mice (5–7 weeks) were purchased from the Jackson Laboratory (Bar Harbor, ME). Breeding pairs of Jα18$^{-/-}$ mice (on C57BL/6 background) provided by Dr. M. Taniguchi (RIKEN Research Center for Allergy & Immunology, Yokohoma, Japan) [15] were bred in a pathogen-free breeding facility at LSUHSC-Shreveport [16]. All mice used in this study were continuously fed standard chow pellet diet, drinking water *ad libitum* and were maintained on a 12h light/dark cycle. All experiments were performed in accordance with NIH guidelines and approved by LSUHSC-Shreveport Animal Care and User Committee.

Reagents

Acetaminophen (APAP; *N*-acetyl-*p*-aminophenol), DL-buthionine-[*S,R*]-sulfoximine (BSO), PBS, perchloric acid and protease cocktail inhibitor were all purchased from Sigma-Aldrich (St. Louis, MO). PVDF membrane and ECL western blotting reagent were purchased from Thermo Fisher Scientific (Rockford, IL) whereas ALT commercial kit was supplied by Thermo Electron (Waltham). Primary antibodies, malondialdehyde pAb and 3-nitrotyrosine mAb, were purchased from EMD (Darmstadt, DE) and Invitrogen (Camarillo, CA), respectively. GAPDH mAb was procured from Santa-Cruz Biotech (Santa Cruz, CA) and anti-mouse horseradish peroxidase secondary antibody was acquired from BD Bisociences (San Diego, CA). *In Situ* Cell Death Detection and Protein Assay kits were obtained from Roche Applied Science (Indianapolis, IN) and Bio-Rad Laboratories (Hercules, CA), respectively.

APAP hepatotoxicity and in vivo treatment protocol

Freshly prepared APAP (600mg/kg, i.p.) in warm sterile PBS was administered to fed mice. Control mice received an equivalent volume of warm sterile PBS. At indicated time-points, mice were anesthetized with a mixture of xylazine and ketamine hydrochloride and blood serum were collected. Livers were then perfused with ice-cold sterile PBS (to remove blood elements) and harvested for the experimental assays described below. For hepatic GSH depletion, mice were administered BSO (500mg/kg, i.p.) or sterile PBS, 2h before APAP and 3h thereafter until termination of the experiment to sustain GSH depletion [17].

Biochemical and histological liver injury

Acute liver injury was determined biochemically by measuring serum levels of the liver enzyme, alanine aminotransferase (ALT), using a commercial kit [16, 18]. For histological evaluation, paraffin embedded liver sections (5 μm thick) were deparaffinized, stained with H & E according to standard protocols and then analyzed by light microscopy in a blinded fashion by a pathologist (PAA). The degree of inflammation in the liver and hepatocyte damage was graded as mild, moderate or severe using a combination of the severity of the inflammation, and the degree of hepatocyte degenerative changes including ballooning degeneration, hepatocyte necrosis and frequency of acidophilic bodies [18].

GSH/GSSG analysis

Perfused livers were snap-frozen in liquid nitrogen immediately after excision from mice. Total hepatic GSH was determined by HPLC using a modified protocol of Reed *et. al.* 1980 [19] as we previously described [18, 19].

APAP metabolites analysis

Perfused liver samples were briefly homogenized in cold sterile PBS containing protease cocktail inhibitor and then centrifuged twice at 4°C for 15 mins at 1800g. Supernatants were filtered using a 0.45μm pore syringe filter and stored in −80°C until use. Proteins in liver and serum supernatants were precipitated in 20% perchloric acid at 4°C by centrifugation for 10 mins at 10,000g. Next, APAP metabolites were separated using a Beckman Ultrasphere ODS C18 Reverse Phase column (80A) on a Shimadzu HPLC system as described by Howie *et al.* 1977 [20]. The concentration of APAP metabolites in liver and serum samples were measured based on the APAP standard phenolic ring absorbance at the wavelength of 195nm [20]. Liver protein concentration was determined using preceding protocol.

Western blot analysis

Perfused liver samples were processed and 30μg of protein were assayed in accordance with protocol previously described [18]. Primary antibodies were diluted in 5% milk at the following dilutions: malondialdehyde (1:1000) or nitrotyrosine (1:1000), incubated overnight in a cold room. Next, membranes were washed three times with PBS in Tween-20 and counterstained with corresponding secondary antibodies conjugated to horseradish peroxidase (1:1000). Membranes were visualized using Pierce ECL western blotting reagent and chemiluminescence film. Subsequently, all membranes were stripped in stripping buffer (0.08% mercaptoethanol, 0.5 mM Tris-HCl pH 6.8, 10% SDS) and reprobed with GAPDH mAb (1:1000) to verify equal protein loading in samples.

In situ analysis of liver apoptosis using TUNEL

Paraffin-embedded liver sections were dewaxed in xylene and rehydrated by passage through a graded series of ethanol solutions, and then PBS. Sections were treated with proteinase K (20 μg/ml in 10 mM Tris-HCl, pH 7.4–8.0) at 37°C for 15 min, washed and then stained with fluorescein nucleotide mixture with terminal deoxynucleotidyl transferase (TdT) from *In Situ* Cell Death Detection kit. Sections were viewed and photographed using standard fluorescent microscopic techniques [18].

Statistical Analysis

Student unpaired *t* test was used for the comparison of means between 2 experimental groups. Comparison among three or more experimental groups was performed using a one-way ANOVA, followed by Newman-Keuls post hoc test. A value of $p<0.05$ was considered significant. Densitometric image analysis was performed using ImageJ 1.43u program (NIH). All data are shown as mean ± SEM.

RESULTS

Resistance of Jα18$^{-/-}$ mice to APAP liver toxicity

In preliminary experiments, we found that administration of APAP (600 mg/kg) to fed mice significantly increased liver injury as reflected by elevated serum ALT without causing mice mortality (data not shown). This dose was used in all experiments. Next, we assessed whether the presence of hepatic Vα14*i*NKT cells contribute to the development of APAP hepatotoxicity. In Fig. 1A, we show that APAP administration into WT mice caused a time-dependent significant increase in serum ALT levels at 8 and 24h relative to naïve. In contrast, Jα18$^{-/-}$ mice, which are selectively deficient in Vα14*i*NKT cells [15, 21], were highly resistant to APAP hepatotoxicity as shown by almost complete significant suppression (>80% reduction) of serum ALT at 8 and 24h (Fig. 1A). As expected, normal levels of serum ALT were observed in both naive WT and Jα18$^{-/-}$ mice (Fig. 1A). A representative histological liver section from WT mice at 24h following APAP treatment

revealed extensive hepatocyte apoptosis and necrotic damage compared to livers from Jα18$^{-/-}$ mice which appeared almost normal (Fig. 1B). Interestingly, the absence of Vα14iNKT cells in Jα18$^{-/-}$ mice was also associated with significantly higher GSH production in the liver at 8 and 24h post-APAP contrary to corresponding WT mice (Fig. 1C). It is notable that GSH levels in naïve Jα18$^{-/-}$ mice did not significantly differ from naïve WT mice. In summary, the resistance of Jα18$^{-/-}$ mice to APAP hepatotoxicity is associated with elevated hepatic GSH.

GSH depletion enhances APAP-induced liver damage in Vα14iNKT cells deficient mice

In view of preceding results, we depleted hepatic GSH in Jα18$^{-/-}$ mice prior to APAP administration to see if it enhanced liver injury. BSO, a specific inhibitor targeting the rate determining step in GSH synthesis, was used to deplete hepatic GSH. Hepatic GSH depletion in Jα18$^{-/-}$ mice resulted in enhanced liver injury and mice mortality (60%) following APAP injection relative to any treatment group (Fig. 1D). In parallel, liver sections from these mice exhibited widespread necrosis, severe hemorrhage, and focal steatosis (Fig. 1E). These results suggest a protective role for GSH in the liver of Jα18$^{-/-}$ mice during APAP hepatotoxicity.

Effect of Vα14iNKT cell deficiency on APAP metabolism in the liver

Considering the observed changes in hepatic GSH levels in Jα18$^{-/-}$ mice during APAP hepatotoxicity, we also quantified hepatic APAP and its metabolites. Following APAP administration, we observed a time-dependent decrease in APAP content in the livers of WT and Jα18$^{-/-}$ mice (Fig. 2A). Notably, APAP content in the liver of Jα18$^{-/-}$ mice was significantly lower at 2h compared to corresponding WT mice (Fig. 2A). In parallel, we observed augmented hepatic APAP-GSH levels in Jα18$^{-/-}$ mice at 2h in contrast to corresponding WT mice (Fig. 2B). In Fig. 2C, we also demonstrate that the level of the APAP metabolite, APAP-glucuronide, in the liver of Jα18$^{-/-}$ mice was significantly reduced at both the 1h and 2h time-points relative to corresponding WT mice. No significant changes in hepatic APAP-sulfate levels were observed in the liver of WT and Jα18$^{-/-}$ mice throughout the time-course (Fig. 2D).

Effect of Vα14iNKT cell deficiency on serum APAP and metabolite levels

Jα18$^{-/-}$ mice had significantly lower serum APAP levels at 0.5h and 2h when compared to corresponding WT mice (Fig. 3A). In contrast to our finding in the liver, no significant change in serum APAP-GSH levels was observed in Jα18$^{-/-}$ mice relative to WT mice throughout the time-course (Fig. 3B). When APAP-GSH is transported outside the cell, it undergoes further metabolism and can form APAP-mercapturate at principal sites of acetylation like the kidneys [22]. At 4h post APAP administration, we identified significantly high APAP-mercapturate serum levels in Jα18$^{-/-}$ mice versus corresponding WT mice (Fig. 3C). Serum APAP-glucuronide levels significantly decreased at 0.5h–2h in Jα18$^{-/-}$ mice versus WT mice (Fig. 3D) whereas serum APAP-sulfate levels were significantly reduced in Jα18$^{-/-}$ mice over WT mice at 2h post-APAP administration (Fig. 3E).

DISCUSSION

Vα14iNKT cells are the most abundant innate T lymphocytes in the liver representing 80–90% of the NKT cell population [12]. During inflammatory responses, Vα14iNKT cells are rapidly activated by TCR-dependent and independent mechanisms to release pro-inflammatory cytokines (e.g. IFN-γ, TNF-α) and chemokines (including CCL5, CCL3) [13]. These pathophysiological responses recruit and/or stimulate intrahepatic leukocytes to produce reactive species, ROS and RNS [13, 23, 24]. Consequently, Vα14iNKT cells have

an important immunoregulatory role representing a critical link between the innate and adaptive immune systems. Vα14*i*NKT cells have been implicated in the pathophysiology of many models of liver inflammation and injury mediated by ischemia/reperfusion [21], microbes [24], alcohol [25] and adenovirus [16]. The specific contribution of Vα14*i*NKT cells to the development of APAP-mediated liver injury is incompletely defined.

In the current study, we provide proof-of-principle that highlights a central role for Vα14*i*NKT cells in suppressing GSH formation in the liver to promote the development of APAP hepatotoxicity. We initially demonstrated that mice deficient in Vα14*i*NKT cells were resistant to liver injury after APAP administration since biochemical and histological markers of liver injury were significantly reduced (>80%) relative to the levels in WT mice. This observation is in contrast to a previous report [10] using the CD1d$^{-/-}$ mice, which are deficient in both Vα14*i*NKT cells and Type II NKT cells. Specifically, CD1d$^{-/-}$ mice were found to be equally susceptible to liver injury as the corresponding WT mice following APAP administration [10]. Interestingly, liver injury in these mice were only alleviated if NK cells were also depleted [10]. NKT and NK cells are known to share similar phenotypic and functional characteristics including cell surface markers, cytokine production and cytotoxicity [10, 13]. Therefore, it has been suggested that the deficiency of either NKT or NK cells could be compensated by the cell type present to induce hepatocyte death during APAP intoxication. However, our study undeniably revealed a novel and essential pathophysiological role for Vα14*i*NKT cells in promoting APAP hepatotoxicity. Next, we evaluated why Vα14*i*NKT cell deficient mice, Jα18$^{-/-}$ mice, were resistant to APAP liver toxicity. We speculated that high GSH levels in Jα18$^{-/-}$ mice relative to WT mice may underlie the hepatoprotective effects documented in Jα18$^{-/-}$ mice following APAP administration. It is notable that GSH is an effective and potent ROS and RNS scavenger shown to suppress/prevent APAP hepatotoxicity [2, 26]. Indeed, we documented elevated hepatic levels of GSH in Jα18$^{-/-}$ mice versus WT mice post-APAP administration. Additionally, we specifically established a hepatoprotective role for hepatic GSH in Jα18$^{-/-}$ mice post-APAP treatment since depletion of hepatic GSH in Jα18$^{-/-}$ mice using BSO significantly exacerbated liver damage (~8-fold) and caused mortality (60%) over APAP-treated Jα18$^{-/-}$ mice administered vehicle. Taken together, we propose that Vα14*i*NKT cells deficiency positively regulate GSH production in the liver to dampen APAP liver toxicity in Jα18$^{-/-}$ mice.

Given that hepatic GSH induced a hepatoprotective in Jα18$^{-/-}$ mice, we next measured APAP and its metabolites to assess any changes in APAP metabolism. We observed a significant increase in hepatic APAP-GSH and serum APAP-mercapturate levels during Vα14*i*NKT cells deficiency that correlated with a significant decrease in APAP levels in Jα18$^{-/-}$ mice compared to the WT mice. Our results indicate that hepatic GSH detoxify APAP metabolites during Vα14*i*NKT cells deficiency thereby reducing liver damage in Jα18$^{-/-}$ mice. Differences between GSH and APAP-related conjugate levels at early time-points as seen in WT and Jα18$^{-/-}$ mice can result from hepatic protein glutathionylation in centrilobular region and biliary excrement [27, 28]. For this reason, we also assessed APAP-glucuronide and APAP-sulfate levels. Glucuronyl transferase activity is known to be regulated by signaling pathways (e.g. Nrf2, PKC, MAPK) during APAP intoxication [29, 30]. We observed a significant decrease in serum and hepatic APAP-glucuronide levels Jα18$^{-/-}$ mice compared to WT mice. In addition, serum but not hepatic APAP-sulfate levels were significantly decreased in Jα18$^{-/-}$ mice versus WT mice. Our data suggests that Jα18$^{-/-}$ mice have a decreased dependency to form APAP-sulfate in extrahepatic tissues like the kidneys [4, 22]. On the basis of these findings, we propose that the enrichment of GSH in the liver of Jα18$^{-/-}$ mice due to a deficiency in Vα14*i*NKT cells was related to a shift in APAP metabolism in favor of GSH conjugation to NAPQI that suppressed liver damage.

GSH is known to effectively scavenge ROS and RNS through enzymatic (e.g. GSH peroxidase) and non-enzymatic reactions that minimizes oxidative and nitrosative stress as well as liver toxicity in response to APAP administration [2, 26]. In agreement, GSH depletion in Jα18$^{-/-}$ mice using BSO during APAP hepatotoxicity enhanced oxidative stress (i.e. MDA-protein adducts), nitrosative stress (i.e. nitrotyrosine) and liver necrosis. Conversely, high GSH levels in Jα18$^{-/-}$ mice due to Vα14iNKT cells deficiency was associated with significantly reduced oxidative stress and DNA fragmentation linked to a decrease in liver damage relative to WT mice with similar treatments. All APAP treatments had high levels of nitrotyrosine staining, which is a reliable footprint of peroxynitrite [2, 8, 31]. Intriguingly, MDA and nitrotyrosine-protein adducts (~60–200kDa) have been reported to resemble albumin monomers and aggregates suggesting that the blood components form adducts with products of reactive species [32, 33]. RNS can elicit DNA fragmentation and is known to inhibit P450 enzymes, caspases, and cytochrome oxidase [34]. This ability of RNS to inhibit caspase activity associates with the lack of DNA fragmentation during GSH depletion accompanying APAP hepatotoxicity.

In summary, our results revealed that Vα14iNKT cells exert pro-inflammatory and pathophysiological responses during APAP hepatotoxicity by suppressing hepatic GSH formation to alter APAP metabolism. Specifically, mice deficient in Vα14iNKT cells had high hepatic GSH levels that detoxified NAPQI to attenuate oxidative stress and the development of liver necrosis.

Supplementary Material

Refer to Web version on PubMed Central for supplementary material.

Acknowledgments

References

1. Larson AM. Acetaminophen hepatotoxicity. Clinics in Liver Disease. 2007; 11:525–48. vi. [PubMed: 17723918]

2. Hinson JA, Roberts DW, James LP. Mechanisms of Acetaminophen-induced Liver Necrosis. Handb Exp Pharmacol. 2010; 196:369–405. [PubMed: 20020268]

3. Wu Z, Han M, Chen T, Yan W, Ning Q. Acute liver failure: mechanisms of immune-mediated liver injury. Liver Int. 2010; 30:782–94. [PubMed: 20492514]

4. Liu L, Klaassen CD. Different Mechanism of Saturation of Acetaminophen Sulfate Conjugation in Mice and Rats. Tox Appl Pharm. 1996; 139:128–34.

5. Wang X, Lu Y, Cederbaum AI. Induction of Cytochrome P450 2E1 Increases Hepatotoxicity Caused by Fas Agonistic Jo2 Antibody in Mice. Hepatology. 2005; 42:400–10. [PubMed: 16025513]

6. Hanawa N, Shinohara M, Saberi B, Gaarde WA, Han D, Kaplowitz N. Role of JNK translocation to mitochondria leading to inhibition of mitochondria bioenergetics in acetaminophen-induced liver injury. J Biol Chem. 2008; 283:13565–77. [PubMed: 18337250]

7. Ishida Y, Kondo T, Ohshima T, Fujiwara H, Iwakura Y, Mukaida N. A pivotal involvement of IFN-gamma in the pathogenesis of acetaminophen-induced acute liver injury. FASEB J. 2002; 16:1227–36. [PubMed: 12153990]

8. Michael SL, Pumford NR, Mayeux PR, Niesman MR, Hinson JA. Pretreatment of mice with macrophage inactivators decreases acetaminophen hepatotoxicity and the formation of reactive oxygen and nitrogen species. Hepatology. 1999; 30:186–95. [PubMed: 10385655]

9. Numata K, Kubo M, Watanabe H, Takagi K, Mizuta H, Okada S, et al. Overexpression of suppressor of cytokine signaling-3 in T cells exacerbates acetaminophen-induced hepatotoxicity. J Immunol. 2007; 178:3777–85. [PubMed: 17339476]

10. Liu ZX, Govindarajan S, Kaplowitz N. Innate immune system plays a critical role in determining the progression and severity of acetaminophen hepatotoxicity. Gastroenterology. 2004; 127:1760–74. [PubMed: 15578514]

11. Masson MJ, Carpenter LD, Graf ML, Pohl LR. Pathogenic role of natural killer T and natural killer cells in acetaminophen-induced liver injury in mice is dependent on the presence of dimethyl sulfoxide. Hepatology. 2008; 48:889–97. [PubMed: 18712839]

12. Eberl G, Lees R, Smiley ST, Taniguchi M, Grusby MJ, MacDonald HR. Tissue-specific segregation of CD1d-dependent and CD1d-independent NK T cells. J Immunol. 1999; 162:6410–9. [PubMed: 10352254]

13. Matsuda JL, Mallevaey T, Scott-Browne J, Gapin L. CD1d-restricted iNKT cells, the 'Swiss-Army knife' of the immune system. Current Opinion in Immunology. 2008; 20:358–68. [PubMed: 18501573]

14. Godfrey DI, MacDonald HR, Kronenberg M, Smyth MJ, Van Kaer L. NKT cells: what's in a name? Nature Reviews. 2004; 4:231–7.

15. Cui J, Shin T, Kawano T, Sato H, Kondo E, Toura I, et al. Requirement for Valpha14 NKT cells in IL-12-mediated rejection of tumors. Science. 1997; 278:1623–6. [PubMed: 9374462]

16. Ajuebor MN, Chen Q, Strieter RM, Adegboyega PA, Aw TY. V(alpha)14iNKT cells promote liver pathology during adenovirus infection by inducing CCL5 production: implications for gene therapy. Journal of Virology. 2010; 84:8520–9. [PubMed: 20573836]

17. Shen HM, Ding WX, Ong CN. Intracellular glutathione is a cofactor in methylseleninic acid-induced apoptotic cell death of human hepatoma HEPG(2) cells. Free Radical Biology & Medicine. 2002; 33:552–61. [PubMed: 12160937]

18. Downs I, Liu J, Adegboyega PA, Aw TY, Ajuebor MN. The ROS Scavenger NAC Regulates Hepatic Vα14iNKT Cells Signaling during Fas mAb-dependent Fulminant Liver Failure. PLoS ONE. 2012; 7:1–11.

19. Reed DJ, Babson JR, Beatty PW, Brodie AE, Ellis WW, Potter DW. High-performance liquid chromatography analysis of nanomole levels of glutathione, glutathione disulfide, and related thiols and disulfides. Anal Biochem. 1980; 106:55–62. [PubMed: 7416469]

20. Howie D, Adriaenssens PI, Prescott LF. Paracetamol metabolism following overdosage: application of high performance liquid chromatography. J Pharm Pharmacol. 1977; 29:235–7. [PubMed: 17674]

21. Arrenberg P, Maricic I, Kumar V. Sulfatide-mediated activation of type II natural killer T cells prevents hepatic ischemic reperfusion injury in mice. Gastroenterology. 2011; 140:646–55. [PubMed: 20950612]

22. Hinchman CA, Matsumoto H, Simmons TW, Ballatori N. Intrahepatic conversion of a glutathione conjugate to its mercapturic acid. Metabolism of 1-chloro-2,4-dinitrobenzene in isolated perfused rat and guinea pig livers. J Biol Chem. 1991; 266:22179–85. [PubMed: 1939239]

23. Nakashima H, Kinoshita M, Nakashima M, Habu Y, Shono S, Uchida T, et al. Superoxide produced by Kupffer cells is an essential effector in concanavalin A-induced hepatitis in mice. Hepatology. 2008; 48:1979–88. [PubMed: 18942689]

24. Ohtaki H, Ito H, Ando K, Ishikawa T, Saito K, Imawari M, et al. Valpha14 NKT cells activated by alpha-galactosylceramide augment lipopolysaccharide-induced nitric oxide production in mouse intra-hepatic lymphocytes. Biochem Biophys Res Commun. 2009; 378:579–83. [PubMed: 19056341]

25. Minagawa M, Deng Q, Liu ZX, Tsukamoto H, Dennert G. Activated natural killer T cells induce liver injury by Fas and tumor necrosis factor-alpha during alcohol consumption. Gastroenterology. 2004:126.

26. Saito C, Zwingmann C, Jaeschke H. Novel mechanisms of protection against acetaminophen hepatotoxicity in mice by glutathione and N-acetylcysteine. Hepatology. 2010; 51:246–54. [PubMed: 19821517]

27. Chen C, Hennig GE, Manautou JE. Hepatobiliary excretion of acetaminophen glutathione conjugate and its derivatives in transport-deficient (TR-) hyperbilirubinemic rats. Drug Metabolism and Disposition: the Biological Fate of Chemicals. 2003; 31:798–804. [PubMed: 12756215]

28. Yang XGJAA, Shi Q, Roberts DW, Hinson JA, Muskhelishvili L, Beger R, Pence LM, Ando Y, Sun J, Davis K, Salminen WF. Changes in Mouse Liver Protein Glutathionylation after Acetaminophen Exposure. J Pharmacol Exp Ther. 2011; 340:360–369. [PubMed: 22045778]

29. Enomoto A, Itoh K, Nagayoshi E, Haruta J, Kimura T, O'Connor T, et al. High sensitivity of Nrf2 knockout mice to acetaminophen hepatotoxicity associated with decreased expression of ARE-regulated drug metabolizing enzymes and antioxidant genes. Toxicol Sci. 2001; 59:169–77. [PubMed: 11134556]

30. Volak L, Court M. Role for protein kinase C delta in the functional activity of human UGT1A6: implications for drug-drug interactions between PKC inhibitors and UGT1A6. Xenobiotica. 2010; 40:306–18. [PubMed: 20196639]

31. Burney S, Caulfield JL, Niles JC, Wishnok JS, Tannenbaum SR. The chemistry of DNA damage from nitric oxide and peroxynitrite. Mutat Res. 1999; 424:37–49. [PubMed: 10064848]

32. Houglum K, Filip M, Witztum JL, Chojkier M. Malondialdehyde and 4-hydroxynonenal protein adducts in plasma and liver of rats with iron overload. J Clin Invest. 1990; 86:1991–8. [PubMed: 2123889]

33. Wayenberg JL, Ransy V, Vermeylen D, Damis E, Bottari SP. Nitrated plasma albumin as a marker of nitrative stress and neonatal encephalopathy in perinatal asphyxia. Free Radical Biology & Medicine. 2009; 1:975–82. [PubMed: 19591921]

34. Chen T, Zamora R, Zuckerbraun B, Billiar TR. Role of nitric oxide in liver injury. Curr Mol Med. 2003; 3:519–26. [PubMed: 14527083]

Highlights

1. Vα14*i*NKT cell deficiency attenuates APAP hepatotoxicity by increasing GSH levels.

2. GSH detoxifies APAP metabolites to alleviate oxidative stress and liver injury.

3. APAP metabolism in Jα18$^{-/-}$ mice was altered in favor of hepatic GSH conjugates.

4. Our study established a unique association between hepatic innate immunity & GSH.

5. APAP metabolism is altered by Vα14*i*NKT cells deficiency to suppress liver damage.

Fig. 1.
Time course for APAP hepatotoxicity in Jα18$^{-/-}$ mice and WT mice. (A) Serum ALT
levels. (B) Representative H & E staining of liver sections from WT and Jα18$^{-/-}$ mice. (C)
HPLC measurement of hepatic GSH levels in WT and Jα18$^{-/-}$ mice before and after APAP
treatment. Data in (A) and (C) are presented as mean ± SEM with n=6–12 mice/group with
*p<0.05 vs. naïve WT; #p<0.05 vs. corresponding WT as assessed by ANOVA/Newman-
Keuls post hoc test. (D–E) Effect of GSH depletion on APAP liver toxicity in Jα18$^{-/-}$ mice.
BSO or PBS was injected in WT and Jα18$^{-/-}$ mice (see methods) for assessment of serum
ALT levels (D) and Histological injury by H & E staining of liver sections (E). Data in D is

shown as mean ± SEM with n=7–19 mice/group with *$p<0.05$ vs. WT/PBS; [#]$p<0.05$ vs. WT/PBS/APAP; [o]$p<0.05$ vs. Jα18$^{-/-}$/PBS/APAP.
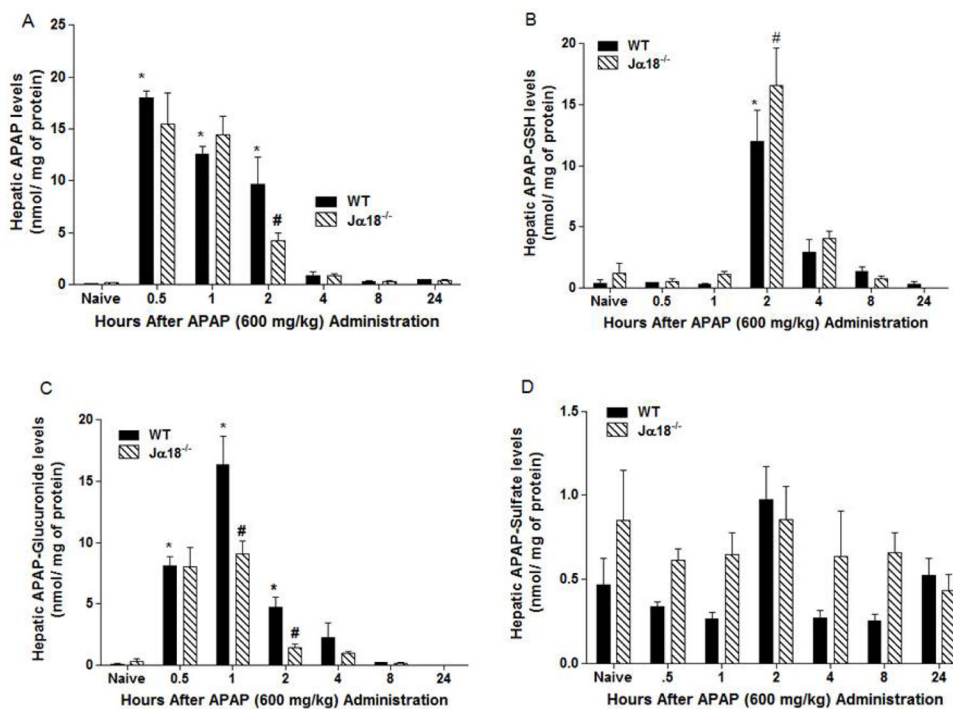
Fig. 2.
Metabolic shift of hepatic APAP and metabolites levels from Jα18−/− mice versus WT mice during APAP liver toxicity. (a) APAP levels. (b) APAP-GSH levels. (c) APAP-Glucuronide levels. (d) APAP-Sulfate levels. All results are presented as mean ± SEM with n=6–12 mice/group; *p<0.05 vs. naïve WT; #p<0.05 vs. corresponding WT.
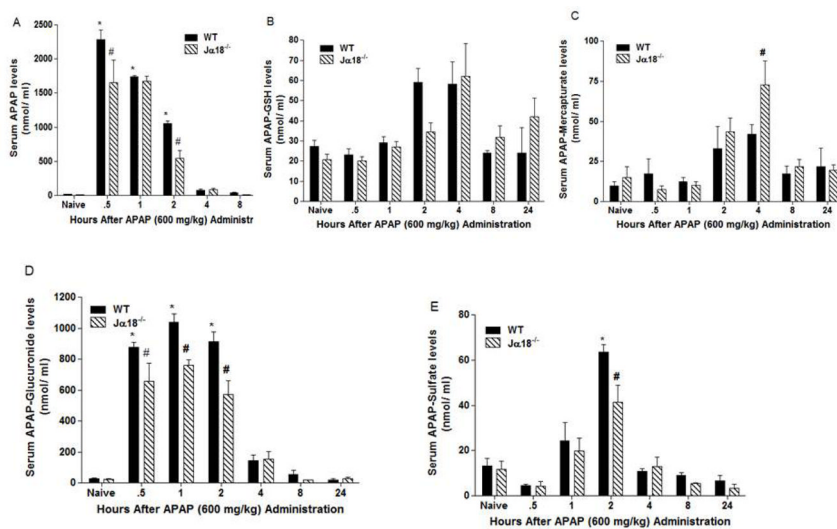
Fig. 3.
Evaluation of serum APAP and metabolites levels in WT and Jα18$^{-/-}$ mice by HPLC during APAP hepatotoxicity. (A) APAP; (B) APAP-GSH; (C) APAP-Mercapturate, (D) APAP-Glucuronide levels and (E) APAP-Sulfate levels. All data are presented as mean ± SEM with n=3–9 mice/group with *p<0.05 vs. naïve WT; #p<0.05 vs. corresponding WT.